Emerg Radiol (2010) 17:299–307
DOI 10.1007/s10140-010-0859-x

ORIGINAL ARTICLE

Thoracic CT findings of novel influenza A (H1N1) infection in immunocompromised patients

Brett M. Elicker · Brian S. Schwartz · Catherine Liu · Eunice C. Chen · Steve A. Miller · Charles Y. Chiu · W. Richard Webb

Received: 4 November 2009 / Accepted: 4 January 2010 / Published online: 29 January 2010

Abstract The goal of this study is to describe the spectrum of initial and follow-up CT findings of novel influenza A (H1N1) infection in a series of immunocompromised patients. Eight immunocompromised patients with documented novel influenza A (H1N1) had CT imaging at our institution between May 2009 and August 2009. A total of 20 CTs (initial and follow-up) were reviewed for the presence, severity, and distribution of the following: ground glass opacity, consolidation, interlobular septal thickening, mosaic perfusion, airway wall thickening, airway dilatation, nodules, cysts, pleural effusion, pericardial effusion, lymphadenopathy, and air trapping. The most common findings were airway thickening/dilatation, peribronchial ground glass opacity, centrilobular nodules, and tree-in-bud opacities. Peripheral consolidation involving the lower lobes was also a common pattern. Findings frequently involved all lobes and were closely associated with either large or small airways. Two patients presented with atypical CT findings including focal lobar consolidation and patchy lower lobe consolidation with soft tissue centrilobular nodules. Most survivors showed near complete resolution of findings within 35 days. CT scans in immunocompromised patients with novel influenza H1N1 commonly show a strong airway predominance of findings or peripheral areas of consolidation involving the lower lobes. A subset of patients with novel influenza A (H1N1) will show findings not typical of viral infection.

Keywords H1N1 · Influenza · Lung infection · Immunocompromise

B. M. Elicker (✉) · W. R. Webb
Department of Radiology and Biomedical Imaging,
University of California, San Francisco,
505 Parnassus Avenue, P. O. Box 0628, San Francisco,
CA 94143, USA
e-mail: brett.elicker@radiology.ucsf.edu

B. S. Schwartz · C. Liu
Division of Infectious Diseases,
University of California, San Francisco,
513 Parnassus Ave., S-380, San Francisco, CA 94143, USA

E. C. Chen · S. A. Miller · C. Y. Chiu
Department of Laboratory Medicine and Infectious Diseases,
University of California, San Francisco,
185 Berry Street, Suite 290, P. O. Box 0100, San Francisco,
CA 94107, USA

Introduction

Influenza poses a continual viral pandemic threat to humans because of its ability to change its antigenic surface proteins and the presence of an animal reservoir. It is hypothesized that influenza has the potential to infect up to 30% of the world's population within a few months [1]. The first case of infection with the novel influenza A (H1N1) strain was detected in March 2009 [2]. Thought to originate in Mexico, 2009 novel influenza A (H1N1) has become the current dominant strain in the USA and other countries. As of October 17, 2009, there were more than 414,000 cases and 5,000 deaths reported worldwide according to the World Health Organization [3]. Knowledge of the clinical implications of novel influenza A (H1N1) strain has been limited by a general lack of information about its virulence, the most susceptible at-risk populations, and effectiveness of immunization regimens.

Influenza causes significant morbidity and mortality in immunocompromised patients with frequent progression to lower respiratory tract disease, particularly in hematopoietic stem cell transplant recipients [4]. In a recent study of

patients with novel influenza A (H1N1) infection requiring hospitalization, immunosuppressed patients comprised 19% of all adults [5]. The clinical and radiographic manifestations of infection in immunocompromised hosts may differ from normal hosts due to an alteration in host altered immunity and a blunted inflammatory response [6, 7]. The goal of this paper is to describe the chest CT findings of novel influenza A (H1N1) infection in a case series of immunocompromised patients and to delineate the natural history of disease on serial follow-up CT scans. A better understanding of the variability of radiographic presentations of novel influenza A (H1N1) infection in immunocompromised hosts will hopefully enable physicians to obtain early identification of infection and treatment.

Materials and methods

Patients

This case series study was approved by our institutional review board, and informed consent was waived. The study population consisted of eight immunocompromised patients who were diagnosed with 2009 novel influenza A (H1N1) strain at the University of California, San Francisco Medical Center and San Francisco General Hospital between May 2009 and August 2009 and also had chest CTs. All study patients tested positive for 2009 novel influenza A (H1N1) by PCR and confirmatory sequencing of the hemagglutinin and neuraminidase genes. Three had stem cell transplantation and three had solid organ transplantation. Demographics and characteristics of the eight patients are shown in Table 1.

Six patients acquired their infections in the community and two had a hospital-acquired infection. All patients were evaluated for other respiratory viral infections, and some patients underwent additional microbiological evaluation for bacterial and fungal infections. Although antibiotic therapy was given in most cases, no significant bacterial or other viral pathogens were recovered.

Testing for 2009 novel influenza A (H1N1)

Respiratory samples from the study patients were identified as positive for influenza by viral direct fluorescent antibody (D^3-DFA Respiratory Virus Screening and ID Kit, Diagnostics Hybrids, Inc.) and/or multiplex PCR testing (Respiratory Viral Panel Test, Luminex Corp). A PCR-based assay was developed for specific detection of the novel influenza A (H1N1) strain and exclusion of other influenza strains, namely six different seasonal H3N2 strains and seasonal H1N1 (Appendix 1).

CT imaging

Chest CT was performed on either a General Electric (Milwaukee, WI, USA) 16-MDCT or 64-MDCT scanner. A total of 20 CT scans were reviewed in the eight patients. These included 15 standard chest CT studies (12 without contrast, three with intravenous contrast), three high-resolution CT studies, and two pulmonary embolism protocol CT studies. Standard CT was performed using the following parameters: 64 or 16×0.625 mm detectors, 120 kVp, automatic mA adjustment, 2.5-mm section reconstruction. For contrast-enhanced CT, a total of 120 cm^3 of iohexol (Omnipaque; General Electric)

Table 1 Demographics, patient characteristics, and clinical factors in the eight patients with documented 2009 novel influenza A (H1N1)

No.	Age (years)	Comorbid condition	Immunosuppression regimen	Symptoms prior to imaging (days)	Fever	O_2	Intubation	Duration of hospitalization (days)	Outcome
1	58	Allogenic SCT 2006	Prednisone, tacrolimus, mycophenolate mofetil	8	Yes	No	No	3	Survival
2	51	Liver transplant 2002	Prednisone, mycophenolate mofetil	9	Yes	No	No	3	Survival
3	53	Heart transplant 2005	Cellcept, tacrolimus	3	Yes	No	No	5	Survival
4	31	Lung transplant 2003	Prednisone, tacrolimus, mycophenolate mofetil	10	Yes	No	No	2	Survival
5	66	Diabetes, renal failure, peritoneal dialysis		3	Yes	Yes	Yes	21	Died
6	36	Allogenic SCT 2007	Prednisone	7	Yes	No	No	17	Survival
7	43	Autologous SCT 2009	Chemotherapy	1	Yes	Yes	Yes	50	Survival
8	48	HIV, Burkitt's lymphoma	Chemotherapy	3	Yes	Yes	Yes	10	Died

SCT stem cell transplant

350 mg/ml was given intravenously with images obtained after a 90-s delay. High-resolution CT was performed using the following parameters: 2×0.625 mm, sampled 1.25 mm sections at 1-cm intervals in inspiration in both prone and supine positions. Dynamic expiratory images were also performed by obtaining six consecutive CT images at selected levels (aortic arch, carina, and just above diaphragm) at 0.5-s intervals during forced expiration using the same CT parameters. Pulmonary embolism protocol CT was performed in a fashion similar to standard contrast-enhanced CT but with appropriate scan timing and section reconstruction at 1.25 mm. Scans were timed using bolus tracking with an ROI on the main pulmonary artery and a trigger of approximately 200 HU. Contrast injection continued throughout the image acquisition with approximately 60–80 cm^3 of iohexol (Omnipaque) administered per patient.

CT analysis

CT images were reviewed by consensus of two subspecialty-trained thoracic radiologists with an average of 22 years of experience in pulmonary imaging. All images were reviewed on a Picture Archiving and Communication System workstation. The readers recorded the presence of each of the following findings: ground glass opacity, consolidation, interlobular septal thickening, mosaic perfusion, airway wall thickening, airway dilatation, nodules, cysts, and air trapping on the expiratory images. The distribution of consolidation and ground glass opacity in affected regions was described as diffuse, peribronchial, subpleural, or as having no specific distribution with respect to the lung architecture. Nodules were considered centrilobular when they demonstrated all of the following features: sparing of the subpleural interstitium, even spacing from one another, and association with the distal bronchovascular interstitium. The lobes affected by each of these findings were also recorded. The severity of consolidation, ground glass opacity, and nodules was graded as mild, moderate, or severe depending upon the percentage of the lobe affected: mild (<25%), moderate (25–75%), and severe (>75%). The presence of pleural effusions, pericardial effusion, and lymphadenopathy was also recorded.

Results

Overall summary of findings

The findings seen on all 20 CT scans included in this study are shown in Table 2. Of note, this table includes both the eight initial CTs and 12 follow-up examinations. Airway thickening was seen in all patients. The second most frequent finding present was consolidation (17 of 20 CT scans). Consolidation was most commonly peripheral in distribution (10 cases) and demonstrated the involvement of the lower lobes in all but two cases. Ground glass opacity was also commonly seen (13 of 20 cases), typically was either diffuse (seven cases) or peribronchial (six cases) in distribution, and involved all lobes in 12 cases. Centrilobular nodules were present in eight of 20 cases and were both of ground glass opacity (three cases) and soft tissue density (five cases).

Initial CT findings

The initial scan on the eight patients was performed an average of 4.7 (range 1–10 days) days after the onset of symptoms. Most common findings on the initial CT scans are shown in Tables 3 and 4.

Airway wall thickening was seen in all cases. Thickening was typically mild (6/8 cases). Airway dilatation often accompanied thickening and was seen in four of eight cases.

Ground glass opacity (GGO) and consolidation were commonly seen. GGO was detected on four of eight of the initial CT scans and was extensive, involving all lobes in every case. GGO had a peribronchial distribution in three cases (Figs. 1 and 2) and was diffuse in one case. Consolidation (Fig. 3) was seen on five of eight of initial CT scans, was commonly peripheral (3/8), and did not have the same peribronchial predominance (1/8) as GGO. In patients with consolidation, one or both lower lobes were involved in all but one case (Fig. 4). The patient without lower lobe involvement had focal posterior right upper lobe consolidation (Fig. 5). One patient with peribronchial consolidation demonstrated a halo sign in which the consolidation had a peripheral rim of GGO.

Centrilobular nodules were seen on three of eight of the initial scans. In two of these cases, they were of ground glass opacity, while in the other case, they were of soft tissue attenuation (Fig. 6). Tree-in-bud was associated with the CT showing soft tissue centrilobular nodules.

The overall distribution of abnormalities was diffuse in five patients. In the remaining three patients, one had mild airway wall thickening only, one showed isolated focal right upper lobe non-segmental consolidation, and one showed soft tissue centrilobular nodules and consolidation in the lower lobes only.

Mosaic perfusion, air trapping, cysts, lymphadenopathy, and interlobular septal thickening were not significant features in any of the cases.

Follow-up CT findings

A total of 12 follow-up CT studies were obtained in six patients. Of these, two patients showed near complete

Table 2 Summary of the CT findings of novel influenza A (H1N1) of the 20 CT scans analyzed

CT findings	Frequency
Ground glass opacity	13/20 (65%)
Diffuse	7/20 (35%)
Peribronchial	6/20 (30%)
Peripheral	0/20 (0%)
Consolidation	17/20 (85%)
Diffuse	2/20 (10%)
Peribronchial	5/20 (25%)
Peripheral	10/20 (50%)
Centrilobular nodules	8/20 (40%)
Ground glass	3/20 (15%)
Soft tissue	5/20 (25%)
Airway thickening	20/20 (100%)
Airway dilatation	9/20 (45%)
Pleural effusions	7/20 (35%)
Pericardial effusion	3/20 (15%)
Lymphadenopathy	1/20 (5%)
Interlobular septal thickening	0/20 (0%)
Cysts	0/20 (0%)
Overall distribution of findings	
All lobes involved	13/20 (65%)
Upper lobe(s) only	2/20 (10%)
Lower lobe(s) only	5/20 (25%)

Eight of these CTs were initial scans performed after presentation. The remaining 12 scans were follow-up examinations. The number of scans on which the finding was present is given with percentage of affected cases in parentheses

resolution of the initial abnormalities (Fig. 7) on the first follow-up examination. The time interval between the initial and follow-up scans in these patients was both 26 days (28 and 35 days, respectively, after the onset of symptoms).

Four patients showed interval worsening of abnormalities on their first follow-up CT scan. The time interval between the initial and follow-up CT in these patients was 3, 3, 4, and 22 days. Two of these patients survived, and two died of their infection. Of the patients who survived, CT showed overall improvement of findings by days 26 and 49 from their initial CT scan (days 33 and 50 after the onset of symptoms). Progression in both of these patients was manifested by new and increased size of patchy bilateral centrilobular nodules. One patient developed tree-in-bud, which was not present on the initial scan, and one patient developed symmetric perihilar ground glass opacity.

One patient who died of the disease had focal consolidation in the right upper lobe on the initial scan and then demonstrated marked worsening of right upper lobe consolidation, in addition to patchy dependent non-segmental consolidation in the posterior lower lobes. The second patient who died of novel influenza A (H1N1) infection initially presented with extensive patchy bilateral GGO and consolidation involving all lobes. Ten days later, a follow-up CT demonstrated improvement in some of the upper lobe consolidation, but worsening of both diffuse GGO and dependent non-segmental consolidation (Fig. 8).

Discussion

Novel influenza A (H1N1) is a new, swine-origin virus first described in 2009 and has become the current dominant strain, as of late 2009 eclipsing seasonal influenza virus in frequency [8]. Although the most high-risk groups appear to be younger patients [2, 9] and pregnant women [10], immunocompromised patients accounted for almost 20% of adult patients hospitalized with novel influenza A (H1N1) [5]. The mortality rate associated with novel H1N1 influenza is also not clear; however, in one study, 6.5% (58/899) of admitted patients had severe illness, and of those with severe disease, 41.4% died of the infection [11]. The CT findings of novel influenza A (H1N1) have not been well described. The goal of this paper is to delineate the CT findings of this infection in a series of immunocompromised patients.

Table 3 Severity, distribution, and lobar involvement of consolidation and ground glass opacity on the initial CT of patients diagnosed with novel influenza A (H1N1)

No.	GGO			Consolidation		
	Severity	Distribution	Lobes involved	Severity	Distribution	Lobes involved
1	Moderate	Peribronchial	All	N/A	N/A	N/A
2	Mild	Peribronchial	All	Moderate	Peribronchial	Both lower lobes
3	N/A	N/A	N/A	N/A	N/A	N/A
4	N/A	N/A	N/A	Moderate	Peripheral	Left lower lobe
5	Severe	Diffuse	All	Severe	Diffuse	All
6	N/A	N/A	N/A	N/A	N/A	N/A
7	Mild	Peribronchial	All	Mild	Peripheral	Right lower lobe
8	N/A	N/A	N/A	Mild	Peripheral	Right upper lobe

Table 4 Presence, characteristics, and distribution of centrilobular nodules, airway thickening/dilatation, and pleural effusions on the initial CT of patients diagnosed with novel influenza A (H1N1)

No.	Centrilobular nodules			Airways		
	Density	Tree-in-bud	Lobes involved	Thickening	Dilatation	Pleural effusions
1	Ground glass	N/A	All	Mild	Moderate	N/A
2	N/A	N/A	N/A	Moderate	Mild	N/A
3	N/A	N/A	N/A	Mild	N/A	N/A
4	Soft tissue	Yes	Both lower lobes	Mild	Mild	N/A
5	N/A	N/A	N/A	Moderate	N/A	Bilateral
6	Ground glass	N/A	Both lower lobes	Mild	N/A	N/A
7	N/A	N/A	N/A	Mild	Mild	N/A
8	N/A	N/A	N/A	Mild	N/A	N/A

In our study, the most common CT findings of novel influenza A (H1N1) included airway thickening/dilatation, peribronchial or diffuse ground glass opacity, peripheral consolidation involving the lower lobes, and centrilobular nodules. In all but one patient, the distribution of findings was closely associated with large and/or small airways.

Two case series have previously described the CT findings of novel influenza A (H1N1). The first of these papers [12] primarily considered the chest radiographic findings of novel influenza A (H1N1) infection and the presence of pulmonary emboli in patients with severe disease. CTs in these patients revealed diffuse GGO and consolidation and nodular opacities. The demographics of most patients in this study were not reported. The other paper [13] described the findings of novel influenza A (H1N1) in a series of seven patients, three of which had CT scans. Most patients demonstrated patchy ground glass opacity and consolidation with a peribronchovascular and subpleural distribution, resembling organizing pneumonia. Most of the patients in this study had comorbidities (e.g., diabetes, hypertension, and lung transplant), but in general, the degree of immunocompromise was much less compared to the patients in our study.

There are several important differences that distinguish our paper. First, all of our patients were immunocompromised, and all but one were being treated with immunosuppressive regimes for transplant or chemotherapy. The CT abnormalities in our study seemed much less severe than those in the aforementioned papers. It is likely there is a lower threshold for imaging immunocompromised patients, even those with mild or non-specific symptoms. Thus, CT imaging is likely obtained closer to the onset of clinical symptoms in the typical immunocompromised patient. Second, it is well known that viral infection commonly produces extensive regions of either diffuse or localized diffuse alveolar damage (DAD) in late stage cases. It is likely that DAD accounts for a significant component of the CT findings of patchy or extensive ground glass opacity and consolidation reported in other studies. It is possible that immunocompromised patients, at

Fig. 1 A 58-year-old man with novel influenza A (H1N1) and history of allogenic stem cell transplant. Axial maximum intensity projection shows patchy bilateral GGO with a peribronchial distribution. Note the small nodular regions of GGO adjacent to some of the distal vessels (*arrows*)

Fig. 2 A 51-year-old, male, liver transplant recipient with novel influenza A (H1N1). Axial CT demonstrates patchy bilateral GGO and consolidation with a peribronchial distribution. There is also airway thickening associated with these abnormalities

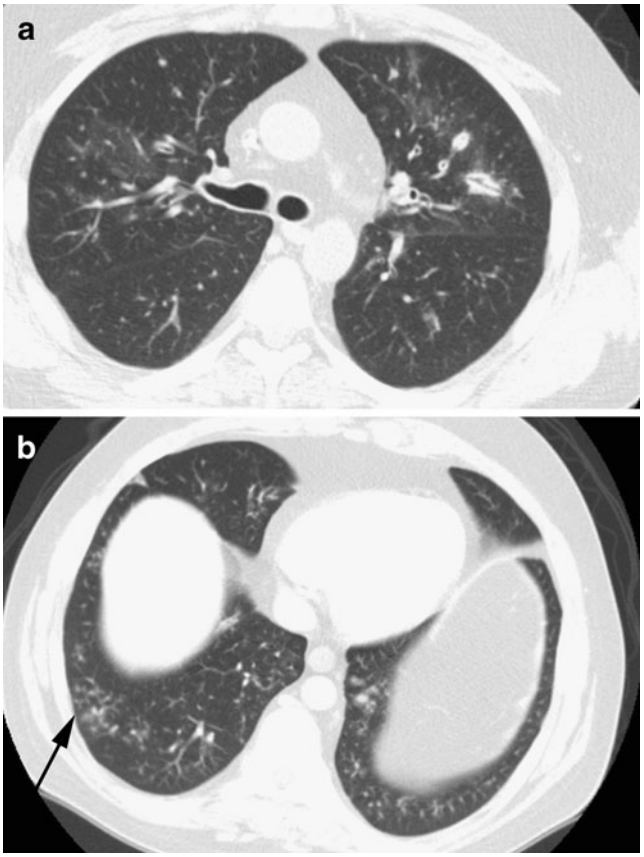

Fig. 3 A 36-year-old man with novel influenza A (H1N1) and Hodgkin's lymphoma s/p autologous stem cell transplant complicated by graft vs. host disease. **a** Axial CT demonstrates patchy bilateral peribronchial consolidation, GGO, centrilobular nodules, and airway thickening typical of the airway-centric nature of novel influenza A (H1N1). The differential density between the central and peripheral lung is due to graft vs. host disease and pre-existed the other acute findings. **b** CT image at the lung base demonstrates patchy soft tissue centrilobular nodules with tree-in-bud opacities (*arrow*)

Fig. 4 A 43-year-old man with novel influenza (H1N1) s/p autologous stem cell transplant. Axial CT demonstrates peripheral posterior bilateral lower lobe consolidation in addition to more diffuse ground glass opacity

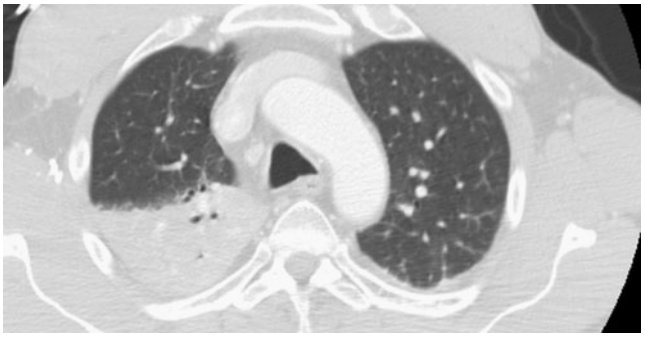

Fig. 5 A 48-year-old man with novel influenza A (H1N1), HIV, and Burkitt's lymphoma. CT demonstrates focal non-segmental right upper lobe consolidation. This was the only significant abnormality detected

least initially, do not develop the same inflammatory response to infection as immunocompetent patients, resulting in less extensive DAD. It is interesting that the patient in our study with the most extensive ground glass opacity and consolidation had significantly less immunocompromise than the remainder of patients.

One CT feature that is unique to our study is the small airway involvement as manifested by centrilobular nodules and tree-in-bud opacities. Three of eight patients demonstrated centrilobular nodules on their initial CT scan, and one of these showed tree-in-bud opacities. One additional patient developed centrilobular nodules and another tree-in-bud opacities on an interval follow-up CT. These small airway findings were distinctly absent in the two other series. It is possible that these small airways abnormalities are obscured later in the disease process when more extensive DAD is present.

Fig. 6 A 31-year-old, female, lung transplant recipient with novel influenza A (H1N1). High-resolution CT scan demonstrates focal soft tissue centrilobular nodules progressing to lobular consolidation within the left lower lobe. While these findings are associated with the distal airways, this finding is more commonly seen with bacterial bronchopneumonia

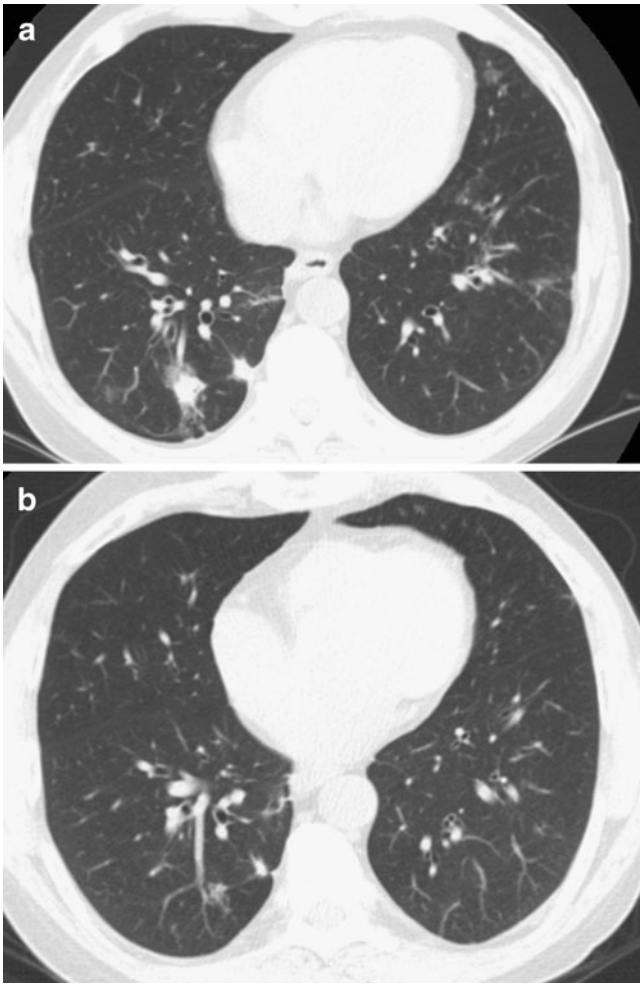

Fig. 7 A 51-year-old, male, liver transplant recipient with novel influenza A (H1N1). **a** Initial CT demonstrates patchy peribronchial consolidation and GGO in the lower lobes. **b** Interval follow-up CT performed 26 days later shows near complete resolution of the previously seen abnormalities

Last, we detected two patients with novel influenza A (H1N1) who demonstrated findings that could easily be confused with bacterial infection. One patient showed patchy, soft tissue centrilobular nodules with segmental consolidation in the lower lobes resembling a bronchopneumonia. Another patient demonstrated focal right upper lobe consolidation that could be confused with a lobar pneumonia. It is very clinically relevant to understand the spectrum of CT findings of novel influenza A (H1N1) including atypical cases. It is likely that a certain percentage of cases will have an appearance not typical of viral infection.

The CT findings of viral infection in general are numerous with previously reported studies demonstrating a myriad of different findings including: consolidation, ground glass opacity, interlobular septal thickening, centrilobular nodules, airway thickening, and air trapping/mosaic perfusion [14, 15]. These findings often overlap with those of other infections such as bacterial, fungal, and mycobacterial disease [16]. Thus, the imaging findings are often non-specific with regards to the offending organism, although CT may be helpful in distinguishing bacterial from atypical organisms [17].

The CT findings of influenza described prior to the emergence of the novel H1N1 strain have not been well documented as most studies have included only a small number of patients or have focused on chest X-rays. The larger studies performed using CT have primarily shown a pattern of extensive or diffuse bilateral GGO and consolidation [18–20].

Our findings are consistent with prior studies of viral infection that have specifically analyzed immunosuppressed patient populations. For instance, Kanne et al. demonstrated

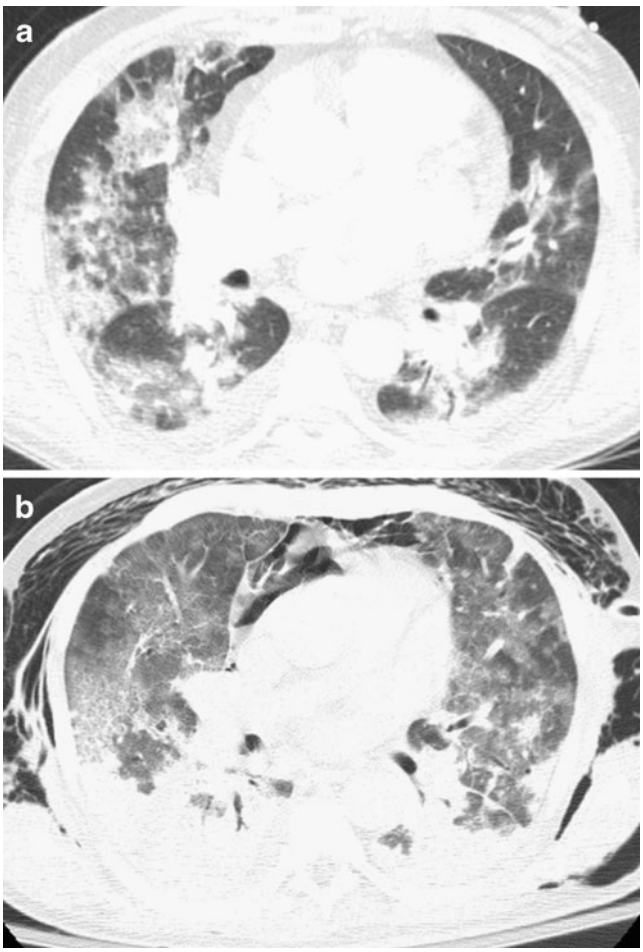

Fig. 8 A 66-year-old man with novel influenza A (H1N1), diabetes, and renal failure. **a** Axial CT demonstrates extensive, patchy bilateral GGO and consolidation without a distinct peribronchial or subpleural distribution. **b** Follow-up CT demonstrates worsening of dependent consolidation, primarily in the lower lobes. While there has been improvement in some of the non-dependent regions of consolidation, the patient has developed more confluent GGO, typical of diffuse alveolar damage. This patient also has pneumomediastinum from alveolar rupture

that the most common CT findings in patients with viral pneumonias in the setting of hematopoetic stem cell transplant were poorly defined centrilobular nodules, and bilateral peribronchial GGO and consolidation [21]. Another study evaluating viral infection in hematopoetic transplant patients, which included five patients with influenza pneumonia, showed that the most common findings were patchy bilateral ground glass opacities, nodules, and thickening of the bronchovascular bundles [22]. In a study looking specifically at influenza infection in the setting of immunosuppression, all three patients who underwent chest CT imaging had GGO, consolidation, and centrilobular nodules with tree-in-bud opacities [23].

Also of interest in our study was the diffuse nature of findings in the majority of patients. A diffuse distribution on imaging is very commonly seen in viral and atypical infections [16]. It is important to note, however, that a subset of patients with novel influenza A (H1N1) will have non-diffuse findings that may simulate infection with other types of organisms. The one patient that did not have diffuse abnormalities was initially thought to have bacterial infection. Infection with influenza is a well-known risk factor for the development of bacterial superinfection. Although the majority of patients were also empirically treated with antibiotic therapy and one cannot completely exclude the possibility of concomitant bacterial infection, no clinically significant bacterial pathogens were isolated from respiratory culture, suggesting that novel influenza A (H1N1) very likely accounted for the radiographic findings in all of these cases.

Progression of disease on serial CTs was most commonly manifested by interval worsening of the airways disease (peribronchial consolidation, airway thickening, and centrilobular nodules) and development of symmetric or diffuse GGO. This later finding is typical of diffuse alveolar damage as a reaction to the viral infection. Of the patients who survived, all but one showed near complete resolution of the findings on interval follow-up CT within 35 days of the onset of clinical symptoms. One patient showed interval improvement at 50 days after the initial CT.

There are several limitations to this study. Firstly, this is small retrospective case series of eight immunocompromised patients, and thus, it is difficult to make definitive statements about the most common manifestations of novel influenza A (H1N1) in general. The goal of this series is simply to describe some of the CT findings that may be seen with this infection and to suggest patterns that may be suggestive of novel influenza A (H1N1) in the appropriate clinical setting. Second, many of the CT scans were done without a high-resolution technique, and thus, precise characterization of abnormalities such as centrilobular nodules is not ideal. With that in mind, standard CT scans, particularly with the routine 2.5-mm reconstructions used at our institution, can assess many of the same findings optimally evaluated with the high-resolution technique. In all cases of nodular disease, we were able to confidently determine that the distribution of nodules was centrilobular despite many of the CTs not being performed with the high-resolution technique. Another limitation is that influenza A infections are not uncommonly complicated by superinfection with other organisms, particularly bacterial. It is possible that some of the findings seen on serial scans performed after the initial diagnosis are due to an infection other than influenza. This is complicated by the fact that many of these patients, because of their immunocompromised state, were also treated empirically with anti-bacterial agents.

In summary, the CT findings of novel influenza A (H1N1) infection in this series of immunocompromised patients tended to be highly airway predominant and most commonly presented with airway thickening/dilatation, peribronchial ground glass, centrilobular nodules, and tree-in-bud opacities. Peripheral consolidation involving the lower lobes was also a common pattern. While these findings can be associated with other infections, they may be suggestive of novel influenza A (H1N1) in the appropriate clinical setting. A high level of suspicion for influenza should be maintained as occasionally it may have an appearance identical to bacterial pneumonia. Most immunocompromised patients with uncomplicated novel influenza A (H1N1) infection show significant radiographic improvement in 35 days or less after the onset of symptoms.

Appendix 1

A PCR-based assay was developed for specific detection of the novel influenza A (H1N1) strain. The hemagglutinin and neuraminidase sequences of 10 seasonal H3N2, seasonal H1N1, and novel H1N1 strains were obtained from GenBank (accession numbers FJ966960, GQ149641, CY047350, GQ895000, and GQ475749 for the hemagglutinin gene and FJ969517, GQ894939, GQ894819, GQ895001, and GQ475750 for the neuraminidase gene) and aligned using ClustalW. Primer sets HA-F-2009H1N1 (5′-GGGTAGCCCCATTGCATTTGGGTAA-3′)/HA-R-2009H1N1 (5′-CCTTTGTTCGAGTCATGATTGGGCC-3′) and NA-F-2009H1N1 (5′-CTGCTGGACAGTCAGTGGTTTCC-3′)/NA-R-2009H1N1 (5′-GCACTTGCTGACCAAGCGACTG-3′) were designed to maximize specificity for

detection of novel influenza A (H1N1) and not the seasonal strains. Total RNA from the samples was extracted using magnetic beads on an automated Biorobot EZ1 instrument (Qiagen Corp) with the Virus 2.0 protocol. RT-PCR for detection of the hemagglutinin and neuraminidase genes of novel H1N1 was performed using the Qiagen 1-Step Kit (Qiagen) according to the manufacturer's protocol. Cycling parameters for PCR were as follows: 15 min of initial denaturation at 94°C followed by 35 cycles of denaturation (30 s at 94°C), annealing (30 s at 50°C), and elongation (30 s at 72°C), with a final extension at 72°C for 8 min. Appropriate positive and negative controls were included with each reaction. Amplified PCR bands of the expected size as visualized on agarose gel electrophoresis were sequenced on an ABI Prism Genetic Analyzer (Elim Biopharmceuticals) to confirm the presence of novel influenza A (H1N1) in samples from seven of the eight study patients. Laboratory confirmation of novel influenza A (H1N1) infection for the one remaining patient was performed at the California Department of Public Health.

References

1. Gatherer D (2009) The 2009 H1N1 influenza outbreak in its historical context. J Clin Virol 45:174–178
2. Perez-Padilla R, de la Rosa-Zamboni D, Ponce de Leon S et al (2009) Pneumonia and respiratory failure from swine-origin influenza A (H1N1) in Mexico. N Engl J Med 361:680–689
3. World Health Organization. Pandemic (H1N1) 2009—update 71. http://www.who.int/csr/don/2009_10_23/en/index.html. Accessed October 26, 2009
4. Nichols WG, Guthrie KA, Corey L, Boeckh M (2004) Influenza infections after hematopoietic stem cell transplantation: risk factors, mortality, and the effect of antiviral therapy. Clin Infect Dis 39:1300–1306
5. Jain S, Kamimoto L, Bramley A et al (2009) Hospitalized patients with 2009 H1N1 influenza in the United States, April–June 2009. N Engl J Med 361:1935–1944
6. Geng E, Kreiswirth B, Burzynski J, Schluger NW (2005) Clinical and radiographic correlates of primary and reactivation tuberculosis: a molecular epidemiology study. JAMA 293:2740–2745
7. Rubin RH (2007) The pathogenesis and clinical management of cytomegalovirus infection in the organ transplant recipient: the end of the 'silo hypothesis'. In: Curr Opin Infect Dis 20:399–407
8. (CDC) CfDCaP (2009) Surveillance for the 2009 pandemic influenza A (H1N1) virus and seasonal influenza viruses—New Zealand, 2009. MMWR Morb Mortal Wkly Rep 58:918–921
9. Kelly HA, Grant KA, Williams S, Fielding J, Smith D (2009) Epidemiological characteristics of pandemic influenza H1N1 2009 and seasonal influenza infection. Med J Aust 191:146–149
10. Jamieson DJ, Honein MA, Rasmussen SA et al (2009) H1N1 2009 influenza virus infection during pregnancy in the USA. Lancet 374:451–458
11. Domínguez-Cherit G, Lapinsky S, Macias A et al (2009) Critically Ill patients with 2009 influenza A(H1N1) in Mexico. JAMA 302:1880–1887
12. Agarwal PP, Cinti S, Kazerooni EA (2009) Chest radiographic and CT findings in novel swine-origin influenza (H1N1) virus (S-OIV) infection. AJR American journal of roentgenology 193:1488–1493
13. Ajlan AM, Quiney B, Nicolaou S, Muller NL (2009) Swine-origin influenza A (H1N1) viral infection: radiographic and CT findings. AJR American journal of roentgenology 193:1494–1499
14. Kang EY, Patz EF Jr, Muller NL (1996) Cytomegalovirus pneumonia in transplant patients: CT findings. J Comput Assist Tomogr 20:295–299
15. McGuinness G, Gruden JF (1999) Viral and pneumocystis carinii infections of the lung in the immunocompromised host. Journal of thoracic imaging 14:25–36
16. Reittner P, Ward S, Heyneman L, Johkoh T, Müller NL (2003) Pneumonia: high-resolution CT findings in 114 patients. Eur Radiol 13:515–521
17. Tanaka N, Matsumoto T, Kuramitsu T et al (1996) High resolution CT findings in community-acquired pneumonia. Journal of computer assisted tomography 20:600–608
18. Bay A, Etlik O, Oner AF et al (2007) Radiological and clinical course of pneumonia in patients with avian influenza H5N1. European journal of radiology 61:245–250
19. Fujita J, Bandoh S, Yamaguchi M, Higa F, Tateyama M (2007) Chest CT findings of influenza virus-associated pneumonia in 12 adult patients. Influenza Other Respi Viruses 1:183–187
20. Qureshi NR, Hien TT, Farrar J, Gleeson FV (2006) The radiologic manifestations of H5N1 avian influenza. Journal of thoracic imaging 21:259–264
21. Kanne JP, Godwin JD, Franquet T, Escuissato DL, Müller NL (2007) Viral pneumonia after hematopoietic stem cell transplantation: high-resolution CT findings. Journal of thoracic imaging 22:292–299
22. Franquet T, Rodriguez S, Martino R, Giménez A, Salinas T, Hidalgo A (2006) Thin-section CT findings in hematopoietic stem cell transplantation recipients with respiratory virus pneumonia. AJR American journal of roentgenology 187:1085–1090
23. Oikonomou A, Müller NL, Nantel S (2003) Radiographic and high-resolution CT findings of influenza virus pneumonia in patients with hematologic malignancies. AJR American Journal of Roentgenology 181:507–511